Raman study of spin–phonon coupling in $ErMnO_3$

2008 J. Phys.: Condens. Matter 20 425219

(http://iopscience.iop.org/0953-8984/20/42/425219)

J. Phys.: Condens. Matter **20** (2008) 425219 (5pp) doi:10.1088/0953-8984/20/42/425219

Raman study of spin–phonon coupling in $ErMnO_3$

J Vermette[1], S Jandl[1] and M M Gospodinov[2]

[1] Département de Physique, Université de Sherbrooke, 2500 Boulevard Université, Sherbrooke, Québec J1K 2R1, Canada
[2] Institute of Solid State Physics, Bulgarian Academy of Sciences, 1784 Sofia, Bulgaria

Received 15 May 2008, in final form 4 September 2008
Published 30 September 2008
Online at stacks.iop.org/JPhysCM/20/425219

Abstract

$ErMnO_3$ single crystals are studied by polarized first-order and second-order micro-Raman measurements as a function of temperature and compared to previous hexagonal $RMnO_3$ (R = Y, Ho, Yb) studies. In addition to the resonance effects of the 684 cm^{-1} mode that are correlated with Mn^{3+} d–d electronic transitions, some phonon frequencies show anomalous temperature variations suggesting a spin–phonon coupling below T_N. The deviation from standard temperature dependence is discussed within a model accounting for the modulation of the exchange interaction by phonon vibrations.

1. Introduction

$RMnO_3$ (R = rare earth) manganites, characterized by strongly correlated electrons, crystallize in the C_{6v}^3 hexagonal space group for R with small ionic radius (R = Ho to Lu) and in the D_{2h}^{16} orthorhombic space group for R with larger radius (R = La to Dy) [1, 2]. The structure-dependent Mn^{3+} electronic level crystal field splittings result in strikingly different physical properties [3, 4]. Colossal magnetoresistance, double-exchange interactions, charge and orbital ordering, as well as simultaneous observation of metallic and ferromagnetic character, have been observed in doped orthorhombic manganites [5–7]. In contrast, the hexagonal manganites are poor conductors and ferroelectrics with relatively high T_c above 500 K [8]. At low temperatures, their Mn^{3+} ion spins ($S = 2$) are coupled by superexchange through the in-plane oxygen ions resulting in spin frustration and an antiferromagnetic arrangement [9–11]. The coexistence of their ferroelectric and magnetic orderings results in a multiferroic promising character for innovative devices.

The temperature-dependent Raman studies of orthorhombic $RMnO_3$ [12, 13] have reported typical A_g mode frequencies (~290 cm^{-1}: octahedra tilt, ~480 cm^{-1}: Jahn–Teller type mode) and B_{2g} mode (~610 cm^{-1}: oxygen breathing mode) and have established significant phonon softening with decreasing temperature below A-type antiferromagnetic ordering [14]. Such phonon frequency renormalization has been attributed to spin–phonon coupling via modulation of the exchange integral [15, 16]. In the hexagonal manganites, phonons with various frequencies between 100 and 700 cm^{-1} have been observed. Raman-active phonons of hexagonal $RMnO_3$ (R = Y, Yb, Ho) have been studied [1, 2, 17, 18] and spin–phonon couplings resulting in marked phonon hardenings at low temperatures have been observed.

Also, in orthorhombic manganites, the origin of the Raman-active excitation at ~650 cm^{-1} and its overtones has been extensively debated. While Saito *et al* [19] argued that these excitations are Γ point orbiton modes, others assigned them to mixed orbiton–phonon character [20–22], multiphonon scattering with dominant roles of the Franck–Condon mechanism [23] or disorder-induced phonon density of states bands [24]. In hexagonal $HoMnO_3$ [2] and $YMnO_3$ [23, 25], second-order Raman scattering has been reported in the 800–1400 cm^{-1} range and assigned to phonon combinations at various points of the Brillouin zone.

The hexagonal manganite $ErMnO_3$ is an interesting multiferroic compound whose dielectric constant exhibits anomalies at the Mn^{3+} spin frustration and Er^{3+} ferrimagnetic transition [8, 9]. While spin frustration ordering occurs below T_N (~80 K) with anisotropic superexchange between Mn^{3+} and Er^{3+} ions [10], the reordering of the antiferromagnetic Mn^{3+} and Er^{3+} ferrimagnetic sublattices could be triggered by external magnetic or electric fields [26]. Like $YMnO_3$ and $LuMnO_3$ that undergo antiferromagnetic transitions with exceptionally large atomic displacements, two orders of magnitude larger than those seen in any other magnetic material [27], $ErMnO_3$ is expected to manifest strong magneto-elastic coupling below T_N.

In this paper we report a micro-Raman study of $ErMnO_3$ as a function of temperature. The objective is to compare

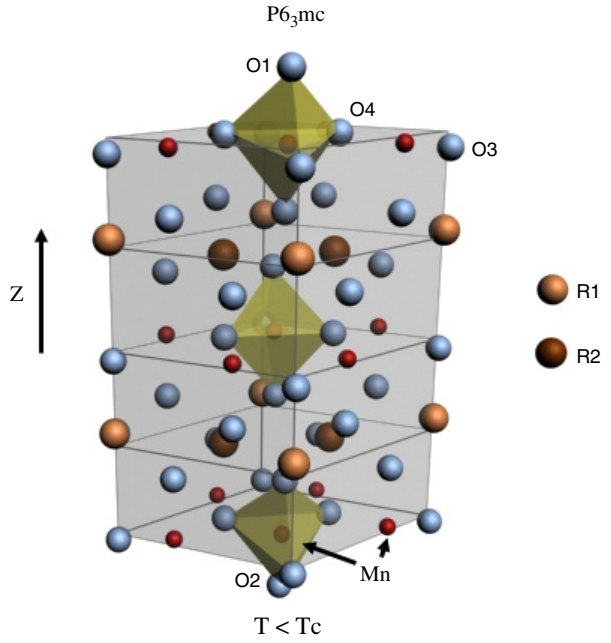

Figure 1. $T < T_c$ crystallographic structure of hexagonal $ErMnO_3$. (This figure is in colour only in the electronic version)

the Raman-active phonon behavior with those of $HoMnO_3$, $YMnO_3$ and $YbMnO_3$ and to evaluate some parameters of the phonon spin coupling in generalization of the Granado *et al* model [15]. Also, second-order Raman scattering and high energy Raman-active modes will be analyzed in comparison with previous studies in various manganites.

2. Experiment

Pure polycrystalline hexagonal $ErMnO_3$ was synthesized by a solid-state reaction of stoichiometric amounts of Er_2O_3 (99.99%) and MnO_2 (99.99%) and annealed for 24 h at 1120 °C in oxygen atmosphere. Then $ErMnO_3$ single crystals were grown by a high temperature solution growth method using $PbF_2/PbO/B_2O_3$ flux [2].

Samples were mounted on the cold finger of a micro-helium Janis cryostat and the Raman spectra were measured in the backscattering configuration using a Labram-800 Raman microscope set-up equipped with a liquid-nitrogen-cooled CCD detector. The exciting laser lines (λ_{exc} = 632.8 nm or 514.5 nm) were focused through a 50× objective with intensity less than 2 mW to avoid crystal heating and structure degradation in manganese oxides [28, 29]. In order to analyze resonance effects and to confirm the overall crystalline quality, a macro-Raman spectrometer (RFS-100) with λ_{exc} = 1064.5 nm was also used. With the incident light parallel to the z axis E_2 and $A_1 + E_2$ Raman-active modes were detected in the $z(xy)\bar{z}$ and $z(xx)\bar{z}$ configurations, respectively.

3. Discussion

At $T < T_c = 830$ K, the non-centrosymmetric $ErMnO_3$ space group is $P6_3cm$. Its hexagonal unit cell ($a = 6.117$ Å and $c = 11.456$ Å [4]) contains six molecular formulas

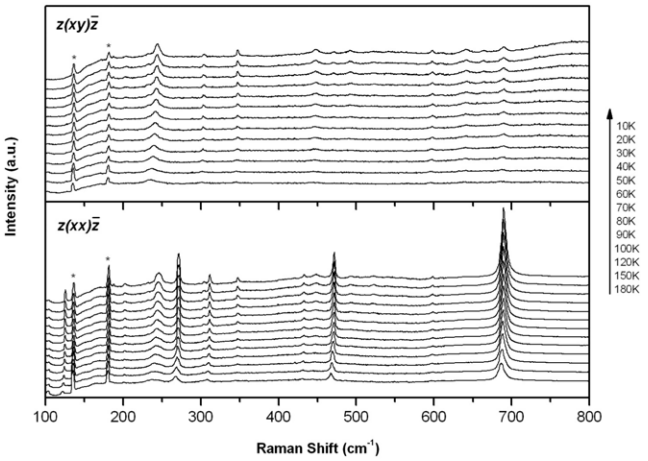

Figure 2. $ErMnO_3$ Raman-active phonons as a function of temperature with $\lambda_{excitation} = 632.8$ nm (intensity of the 684 cm^{-1} has been divided by 6). * indicates plasma lines.

forming tilted MnO_5 bipyramids with O_1, O_2 and O_3, O_4 apical and non-equivalent in-plane oxygen ions, respectively. The erbium ions are located, as shown in figure 1, between the bipyramid layers. Resonance effects are expected for excitations close to the Mn^{3+} d–d electronic transitions [3, 30], and in our experimental configuration, with the incident light parallel to the z axis, 9 A_1 and 15 E_2 Raman-active modes are predicted by group theory for the Γ-point zone-center irreducible representations [1]:

$$\Gamma = 10A_1 + 5A_2 + 10B_1 + 5B_2 + 15E_1 + 15E_2.$$

In figure 2, $ErMnO_3$ A_1 and E_2 Raman-active phonons are shown as a function of temperature. Six A_1 and seven E_2 modes are observed. With decreasing temperature no additional phonons or major changes in the spectral symmetries are observed, confirming the absence of structural phase transitions below $T_N \sim 80$ K. Even if all phonon linewidths narrow while their intensities and frequencies increase, their temperature evolutions differ significantly. For example, as shown in table 1, between 300 K and 10 K, frequency shifts vary from 1 cm^{-1} to 14 cm^{-1} and linewidths from 0.5 to 7.5 cm^{-1} for the 159 cm^{-1} and 234 cm^{-1} E_2 symmetry phonons, respectively. Variations of the A_1 phonon frequency shifts are less marked, typically from 2 to 3 cm^{-1} for the 430 cm^{-1} and 684 cm^{-1} phonons, respectively. Some phonon intensities increase remarkably below T_N (e.g. 684 cm^{-1}), indicating polarizability renormalizations. Resonance effects are also observed when various excitation laser lines are used (figure 3). In particular, with the laser excitation = 1.96 eV, close to the Mn^{3+} d–d electronic transition, additional phonons at 343 and 592 cm^{-1} are observed. Also the intensity of the 684 cm^{-1} phonon, which corresponds to the O_1 and O_2 apical oxygen stretching vibrations along the z axis, is strongly enhanced, confirming the charge transfer ∼1.7 eV between filled d_{xy,x^2-y^2} and empty $d_{3z^2-r^2}$ orbitals [2, 3, 30]. In table 1, $ErMnO_3$ Raman-active phonon frequencies for various atomic displacements are compared to those of $YMnO_3$ [1, 17], $HoMnO_3$ [2] and

Table 1. A_1 and E_2 Raman-active modes in hexagonal manganites. Phonon bandwidths are indicated in brackets.

		$YMnO_3$ [1]	$HoMnO_3$ [2]	$ErMnO_3$ (Present work)		$YbMnO_3$ [18]
Ionic displacements	Mode	300 (K)	300 (K)	300 (K)	10 (K)	15 (K)
z(R)	A_1	148		123 (4.5)	128 (3.5)	121
$+z$(R) $-$ z(Mn)		257	262	266 (10)	272 (4)	261
x(Mn), z(O_3)		297	295	305(8)	313 (4.5)	
$+z$(O_4, O_3) $-$ z(Mn)		433	427	430 (7.5)	432 (4)	434
$+x$, y(O_1, O_2) $-$ x, y(Mn)		459	463	464(7)	470 (4.5)	467
$+z$(O_1) $-$ z(O_2)		681	685	684 (11)	688 (8)	682
x, y(R)	E_2	135	136	138 (7.5)	142 (4.3)	139
x, y(R)				159 (4)	160 (3.5)	161
$+xy$(Mn) $-$ xy(O_3, O_4)		215	221	234 (14)	248 (6.5)	253
z(O_2, O_1), xy(O_4)		302	295	297 (10)	303 (4)	304
$+xy$(O_1, O_2, O_4, O_3) $-$ xy(Mn)				343 (12)	346 (3.5)	
$+xy$(O_4) $-$ xy(O_1, Mn)			442	444 (14)	446 (8.3)	
x, y(O_4, O_3)				592 (7)	597 (6.2)	

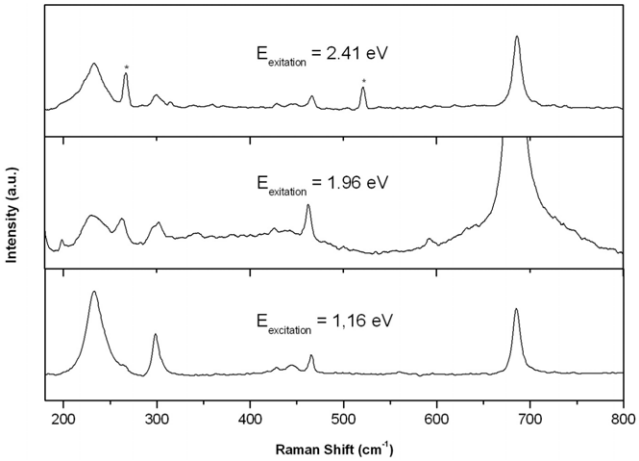

Figure 3. $ErMnO_3$ Raman-active phonons at $T = 300$ K for different excitation energies. * indicates plasma lines.

$YbMnO_3$ [18]. The frequencies of the A_1 (123 and 266 cm^{-1}) phonons corresponding to the rare earth z displacements decrease as the rare earth masses ($m_Y < m_{Ho} < m_{Er} < m_{Yb}$) increase, in contrast to the E_2 (138 and 159 cm^{-1}) phonons which also involve rare earth displacements. The A_1 (305, 430 and 464 cm^{-1}) and E_2 (234, 297 and 444 cm^{-1}) phonons imply displacements of O^{2-} and Mn^{3+} ions and reflect the rare earth dependence of the O^{2-}–Mn^{3+} distances and their corresponding force constants. The A_1 (684 cm^{-1}) phonon that modulates the z-axis-oriented polarization has rather small frequency shifts between room temperature and 10 K (∼3 cm^{-1}) while the E_2 (234 cm^{-1}) phonon frequency that corresponds to displacements of the O_3, O_4 and Mn^{3+} ions in the xy plane increases by ∼14 cm^{-1}.

In figures 4(a)–(c) typical phonon frequency evolutions as a function of temperature are shown. The frequencies of the A_1 (123, 266 and 430 cm^{-1}) phonons, which involve ionic motions along the z axis, increase rather monotonically without anomalies near and below T_N (figure 4(a)). In contrast such anomalies are observed for the E_2 (234, 297 cm^{-1}) phonons which involve atomic motions in the xy plane (figure 4(b)).

Upon assumption of negligible spin–phonon coupling, the temperature dependence of a phonon frequency is mainly governed by the anharmonic decay and in a good approximation follows the relation [31]

$$\omega(T) = \omega_0 - C\left[1 + \frac{2}{e^{\frac{\hbar\omega_0}{2k_B T}} - 1}\right], \tag{1}$$

where ω_0 and C are adjustable parameters. As illustrated in figure 4(a), equation (1) fits well the experimental points for the A_1 phonons at 123, 266 and 430 cm^{-1}. However, in the case of strong spin–phonon coupling one expects deviations from this dependence near and below the magnetic ordering temperature. Obviously this is the case for the experimental results presented in figure 4(b) where phonon frequency shifts should remain constant below $T = 80$ K if only anharmonicity is considered. In order to account for the effect of the spin–phonon coupling on the temperature dependence of the phonon frequency, we follow the approach proposed by Granado *et al* [15], assuming that the extra phonon hardening reflects an additional contribution to the force constants due to the spin–phonon interaction. Representing the modulation of the exchange interaction J_{ij} between two manganese ions by the displacements u_k^α of the kth oxygen ion participating in the α mode as

$$\Delta J_{ij}^\alpha = J_{ij}^0 + \tfrac{1}{2}\sum_k [u_k^\alpha \nabla_k]^2 J_{ij}, \tag{2}$$

the total Hamiltonian becomes

$$H^\alpha = H_{\text{latt}}^\alpha + H_{\text{spin}}^\alpha \approx \underbrace{\sum_k \frac{P_k^2}{2\mu_\alpha} + \frac{1}{2}\sum_k \tilde{K}_k^\alpha (u_k^\alpha)^2}_{H_{\text{latt-spin}}^\alpha} - \underbrace{\sum_{i,j>i} J_{ij}^0 \langle S_i \cdot S_j \rangle}_{H_{\text{spin}}^0}, \tag{3}$$

with μ_α being the effective mass of the α mode, P_k the oxygen ion k momentum and $\tilde{K}_k^\alpha$ the renormalized force constant:

$$\tilde{K}_k^\alpha = K_k^\alpha - \sum_{i,j>i} \nabla_k^2 J_{ij} \langle S_i \cdot S_j \rangle, \tag{4}$$

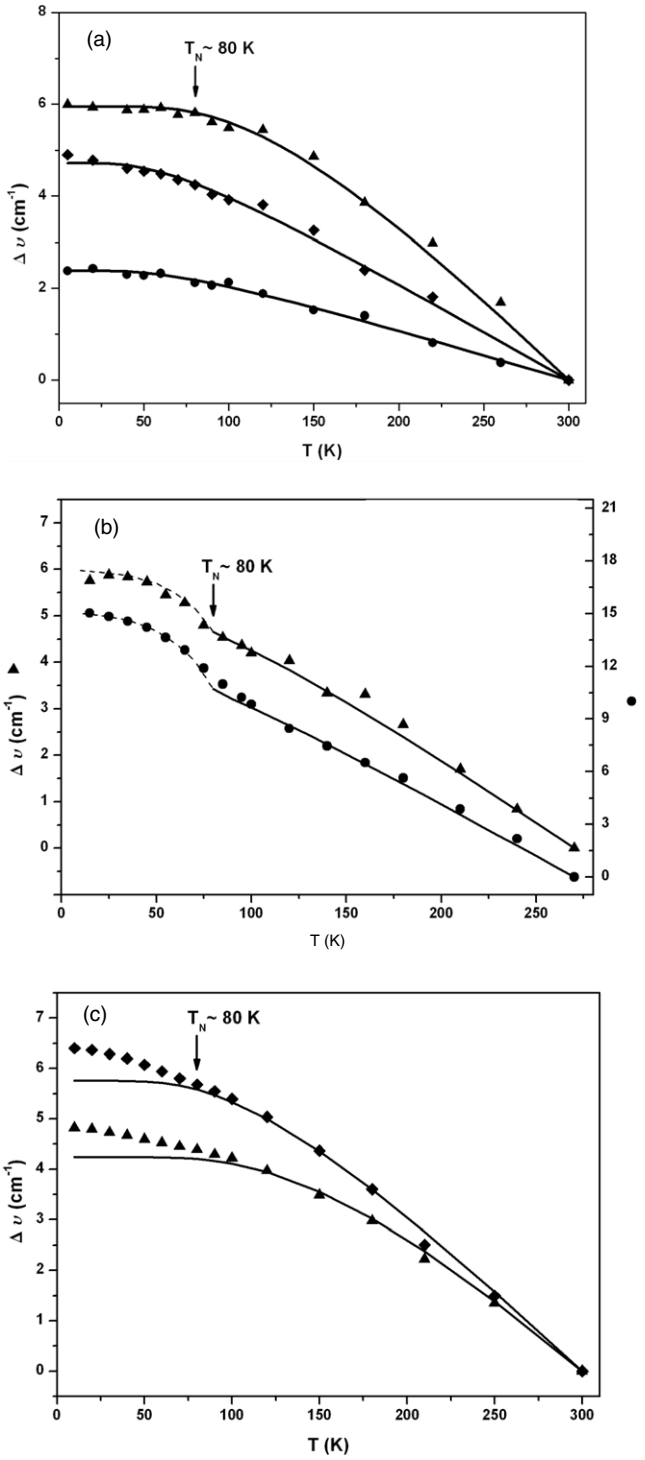

Figure 4. (a) $ErMnO_3$ temperature evolution of A_1 (♦ 123 cm^{-1}; ▲ 266 cm^{-1}; ● 430 cm^{-1}) phonon frequency shifts. Solid lines correspond to anharmonicity predictions. (b) $ErMnO_3$ temperature evolution of E_2 (● 234 cm^{-1}; ▲ 297 cm^{-1}) phonon frequency shifts. Solid and dashed lines correspond to predictions of anharmonicity and spin–phonon interaction, respectively. (c) $ErMnO_3$ temperature evolution of A_1 (♦ 464 cm^{-1}; ▲ 684 cm^{-1}) phonon frequency shifts. Solid lines correspond to anharmonicity predictions.

that corresponds to the phonon energy renormalization:

$$(\Delta\omega_k^{\alpha})_{\mathrm{s-ph}} = -\frac{1}{2\mu_\alpha\omega_k^{\alpha}}\sum_{i,j>i}\nabla_k^2\, J_{ij}\langle S_i\cdot S_j\rangle. \qquad (5)$$

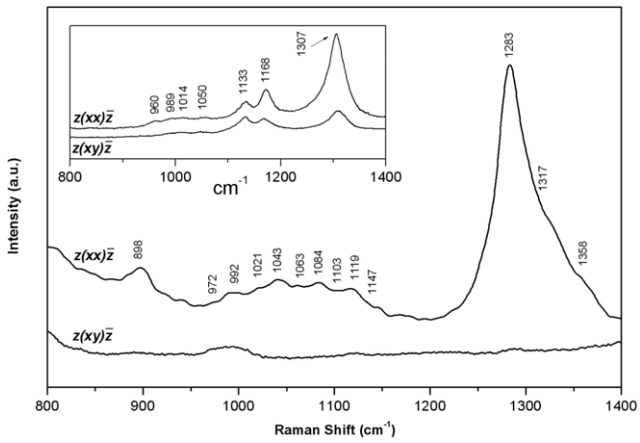

Figure 5. $ErMnO_3$ second-order Raman excitations in the 800–1400 cm^{-1} range. Inset: $SmMnO_3$ second-order excitations [22].

Within this model, the contribution of the spin–phonon interaction, at $T < T_N$, to the phonon frequency shift as a function of temperature is given by

$$(\Delta\omega_\alpha)_{\mathrm{s-ph}} = \frac{3}{m\omega_\alpha}\nabla^2_{\mathrm{O}_{3,4}} J_{x,y}\left[\frac{M(T)}{4\mu_{\mathrm{B}}}\right]^2 \qquad (6)$$

where $M(T)$ corresponds to the temperature-dependent magnetization [11]. This expression can be fitted to the experimental data for the E_2 (234 cm^{-1}) phonon with one adjustable parameter $\nabla^2 J = 8.5$ mRyd $Å^{-2}$ and for the E_2 (297 cm^{-1}) phonon with $\nabla^2 J = 3.5$ mRyd $Å^{-2}$. It is worth noting here that these two phonons involve motions of O_3 and O_4 oxygen atoms within the xy plane. Interestingly, the A_1 (464 and 684 cm^{-1}) phonons, which correspond to O_1 and O_2 vibrations, also deviate below T_N from the pure anharmonicity dependence (see figure 4(c)). The study by Fiebig *et al* of the interaction of frustrated magnetic sublattices in $ErMnO_3$ has concluded that Er–Mn exchange processes dominate the magnetic properties [10]. Since the O_1 and O_2 ions play a bridging role in the superexchange interaction between the Mn^{3+} planes and Er^{3+} planes a renormalization of their vibration frequencies by the antiferromagnetic coupling between the Mn^{3+} planes at 0 and $c/2$ should be expected below T_N.

$ErMnO_3$ second-order Raman excitations are detected in the 800–400 cm^{-1} range with mainly A_1 symmetry (figure 5). Since there is no restriction on individual phonon wavevectors, such excitations reflect the phonon density with a maximum around 1280 cm^{-1}. The positions of the main maxima at ∼874, 1080, 1117, 1280 and 1368 cm^{-1} are practically the same as in hexagonal $HoMnO_3$, indicating a strong similarity between these two compounds' force constants as compared to small differences with the orthorhombic manganites in which second-order Raman excitations are slightly shifted ∼960, 989, 1014, 1050, 1133, 1168 and 1307 cm^{-1} (figure 5 inset [22]).

4. Conclusion

First- and second-order polarized phonon Raman spectra of $ErMnO_3$ single crystals were studied as a function of temperature. The zone-center vibrations are associated with ionic motions predicted by lattice dynamics calculations. Resonance phenomena are observed for the A_1 (684 cm^{-1}) mode intensity governed by the Mn^{3+} ion electronic orbital occupancies. The phonon energy shifts as a function of temperature are analyzed. Below $T_N = 80$ K, some of the phonon frequencies exhibit extra hardening deviations that could not be modeled by anharmonicity alone. The variations with temperature of the E_2 (234 and 297 cm^{-1}) phonon frequencies, which are characterized by ionic locations and vibrations within the Mn^{3+} spin frustration plane, are successfully fitted using a model for the spin–phonon interaction based on modulation of the exchange integrals by ionic vibrations. The temperature dependence of the A_1 (464 and 684 cm^{-1}) phonon frequencies, which are characterized by the two apical oxygen motions, reflects a complex anisotropic superexchange interaction between the Mn^{3+} and the Er^{3+} ions. Finally, the second-order Raman excitations are detected in the 800–1400 cm^{-1} range and compared to orthorhombic manganite excitations.

Acknowledgments

JV and SJ acknowledge support from the National Science and Engineering Research Council of Canada and the Fonds Québécois de la Recherche sur la Nature et les Technologies. The work of MMG is supported by grant no. TK-X-1712/2007 of the Bulgarian Science Fund.

References

[1] Iliev M N, Lee H-G, Popov V N, Abrashev M V, Hamed A, Meng R L and Chu C W 1997 *Phys. Rev.* B **56** 2488
[2] Litvinchuk A P, Iliev M N, Popov V N and Gospodinov M M 2004 *J. Phys.: Condens. Matter* **16** 809
[3] Souchkov A B, Simpson J R, Quijada M, Ishibashi H, Hur N, Ahn J S, Cheong S W, Millis A J and Drew H D 2003 *Phys. Rev. Lett.* **91** 027203
[4] Zhou J-S, Goodenough J B, Gallardo-Amores J M, Morán E, Alario-Franco M A and Caudillo R 2006 *Phys. Rev.* B **74** 014422
[5] Xiong G C, Li Q, Ju H L, Mao S N, Senapati L, Xi X X, Greene R L and Venkatesan T 1995 *Appl. Phys. Lett.* **66** 1427
[6] Zener C 1951 *Phys. Rev.* **81** 440
[7] Khomskii D I and Sawatzky G A 1997 *Solid State Commun.* **102** 87
[8] Iwata N and Kohn K 1998 *J. Phys. Soc. Japan* **67** 3318
[9] Fiebig M, Fröhlich D, Kohn K, Leute S, Lottermoser T, Pavlov V V and Pisarev R V 2000 *Phys. Rev. Lett.* **84** 5620
[10] Fiebig M, Degenhardt C and Pisarev R V 2001 *Phys. Rev. Lett.* **88** 027203
[11] Park J, Kong U, Choi S, Park J-G, Lee C and Jo W 2002 *Appl. Phys.* A **74** S802
[12] Iliev M N, Abrashev M V, Lee H-G, Popov V N, Sun Y Y, Thomsen C, Meng R L and Chu C W 1998 *Phys. Rev.* B **57** 2872
[13] Iliev M N, Abrashev M V, Laverdiere J, Jandl S, Gospodinov M M, Wang Y-Q and Sun Y-Y 2006 *Phys. Rev.* B **73** 064302
[14] Jandl S, Barilo S N, Shiryaev S V, Mukhin A A, Ivanov V Y and Balbashov A M 2003 *J. Magn. Magn. Mater.* **264** 36
[15] Granado E, Garcıa A, Sanjurjo J A, Rettori C, Torriani I, Prado F, Sanchez R D, Caneiro A and Oseroff S B 1999 *Phys. Rev.* B **60** 11879
[16] Laverdiere J, Jandl S, Mukhin A A, Ivanov V Y, Ivanov V G and Iliev M N 2006 *Phys. Rev.* B **73** 214301
[17] Fukumura H, Matsui S, Harima H, Kisoda K, Takahashi T, Yoshimura T and Fujimura N 2007 *J. Phys.: Condens. Matter* **19** 365239
[18] Fukumura H, Hasuike N, Harima H, Kisoda K, Fukae K, Takahashi T, Yoshimura T and Fujimura N 2007 *J. Phys.: Conf. Ser.* **92** 012126
[19] Saitoh E, Okamoto S, Takahashi K T, Tobe K, Yamamoto K, Kimura T, Ishihara S, Maekawa S and Tokura Y 2001 *Nature* **410** 180
[20] Van Den Brink 2001 *J. Phys. Rev. Lett.* **87** 217202
[21] Jandl S, Laverdiere J, Mukhin A, Ivanov V and Balbashov A 2006 *Physica* B **381** 214
[22] Laverdière J, Jandl S, Mukhin A A and Ivanov V Y 2006 *Eur. Phys. J.* B **54** 67
[23] Martín-Carrón L and de Andres A 2004 *Phys. Rev. Lett.* **92** 175501
[24] Iliev M N, Hadjiev V G, Litvinchuk A P, Yen F, Wang Y-Q, Sun Y Y, Jandl S, Laverdiere J, Popov V N and Gospodinov M M 2007 *Phys. Rev.* B **75** 064303
[25] Iliev M N, Hadjiev V G, Litvinchuk A P and Meng R L 2003 *Phys. Rev. Lett.* **90** 069701
[26] Sugie H, Iwata N and Kohn K 2002 *J. Phys. Soc. Japan* **71** 1558
[27] Lee S, Pirogov A, Kang M, Jang K-H, Yonemura M, Kamiyama T, Cheong S-W, Gozzo F, Shin N, Kimura H, Noda Y and Park J-G 2008 *Nature* **451** 805
[28] Julien C, Massot M, Rangan S, Lemal M and Guyomard D 2002 *J. Raman Spectrosc.* **33** 223
[29] Julien C, Massot M and Poinsigon C 2004 *Spectrochim. Acta* A **60** 689
[30] Choi W S, Kim D G, Seo S S A, Moon S J, Lee D, Lee J H, Lee H S, Cho D-Y, Lee Y S, Murugavel P, Yu J and Noh T W 2008 *Phys. Rev.* B **77** 045137
[31] Balkanski M, Wallis R F and Haro E 1983 *Phys. Rev.* B **28** 1928